

Do long-duration GRBs follow star formation?

Dafne Guetta¹ and Tsvi Piran²

¹ Osservatorio astronomico di Roma e.v. Frascati 33 00040 Monte Porzio Catone, Italy

² Racah Institute for Physics, The Hebrew University, Jerusalem 91904, Israel

To be determined

Abstract. We compare the luminosity function and rate inferred from the BATSE long bursts peak flux distribution with those inferred from the Swift peak flux distribution. We find that both the BATSE and the Swift peak fluxes can be fitted by the same luminosity function and the two samples are compatible with a population that follows the star formation rate. The estimated local long GRB rate (without beaming corrections) varies by a factor of five from $0.05 \text{ Gpc}^{-3} \text{ yr}^{-1}$ for a rate function that has a large fraction of high redshift bursts to $0.27 \text{ Gpc}^{-3} \text{ yr}^{-1}$ for a rate function that has many local ones. We then turn to compare the BeppoSax/HETE2 and the Swift observed redshift distributions and compare them with the predictions of the luminosity function found. We find that the discrepancy between the BeppoSax/HETE2 and Swift observed redshift distributions is only partially explained by the different thresholds of the detectors and it may indicate strong selection effects. After trying different forms of the star formation rate (SFR) we find that the observed Swift redshift distribution, with more observed high redshift bursts than expected, is inconsistent with a GRB rate that simply follows current models for the SFR. We show that this can be explained by GRB evolution beyond the SFR (more high redshift bursts). Alternatively this can also arise if the luminosity function evolves and earlier bursts were more luminous or if strong selection effects affect the redshift determination.

Key words. cosmology: observations: gamma rays: bursts

1. Introduction

Gamma ray bursts (GRBs) are one of the most powerful events in the universe. The high energy photons emitted travel from cosmological distance tracing the star formation history in the universe. Our understanding of long ($T_{90} > 2 \text{ sec}$) GRBs and their association with stellar collapse followed from the discovery in 1997 of GRB afterglow and the subse-

quent identification of host galaxies, redshift measurements and detection of associated Supernovae.

However the number of GRBs with a measured redshift is still limited. Only a small fraction of the BeppoSax/HETE 2 bursts have measured redshifts. It was expected that *Swift* would allow further insight into the redshift properties of these objects. Indeed, the ability of *Swift* to locate and follow-up fainter bursts than the previous satellites, has allowed more distant bursts to be studied. The mean redshift of the BeppoSax/HETE 2 sample was $z_{\text{mean}} = 1.4$, while bursts discovered by *Swift* now have $z_{\text{mean}} = 2.8$. However the number of *Swift* bursts with a measured redshift is still small as only 30 bursts out of 130 detected bursts has redshift. The selection effects that arise in both samples are not clear and hard to quantify (Fiore et al. 2006). Therefore, at present we cannot derive directly the GRB luminosity function and rate evolution that are fundamental to understand the nature of these objects.

We can constrain the luminosity function and rate distribution by fitting the BATSE and *Swift* peak flux distributions to those expected for a given luminosity function and GRB rate (Piran 1992, Cohen & Piran 1995, Fenimore & Bloom 1995, Loredo & Wassemann 1995, Horack & Hakkila 1997, Loredo & Wassemann 1998, Piran 1999, Schmidt 1999, Schmidt 2001, Sethi & Bhargavi 2001, Guetta et al. 2005, Guetta & Piran 2005, 2006). However, since the observed flux distribution is a convolution of these two unknown functions we must assume one and find a best fit for the other. We assume that the rate of long bursts follows the star formation rate (or a modification of the star formation rate that allows for an enhancement) and we search for the parameters of the luminosity function. We show, in the first part of the paper that one can obtain a fully consistent fit for both the BATSE and the *Swift* peak flux samples.

A more complicated issue is to compare the observed redshift distribution of BeppoSax/HETE 2 with the observed redshift distribution of *Swift* and with the predictions of the models for the rate and luminosity function that were inferred from the peak flux distribution. We turn to this problem in the second part of the paper. Clearly the intrinsic GRB distribution is the same and the differences between the observed distributions should arise from the differences in thresholds, in the observed energy band and in selection effects that determine the samples of bursts with observed redshifts. Because of the higher detection thresholds the BeppoSax/HETE 2 observed distribution is nearer to us than the *Swift* one. However, the difference in thresholds is not enough to explain the difference between the two observed redshift distributions. With more *Swift* high redshift bursts than expected we conclude that either GRBs evolve faster than the SFR (more high redshift bursts), or that the assumption that the luminosity function is independent of z is wrong. Alternatively different selection determine the distribution of bursts with observed redshifts (Fiore et al. 2006). We also consider models where the GRB rate is a convolution of the SFR and of a sharp jumps to high values at high

redshift. These models could relate to the fact that GRBs seem to be more abundant in low metallicity regions (Fynbo et al., 2003; Vreeswijk et al., 2004). Such a jump could arise, for example, from a low metallicity threshold, below which the GRB rate jumps. Note, however, that a recent analysis of Fynbo et al. (2006) shows that GRBs occur in environments covering a broad range of metallicity at a given redshift.

2. Luminosity function from the BATSE and the Swift samples

Our data set and methodology follows Guetta et al. (2005). For BATSE, we consider all the long GRBs ($T_{90} > 2$ sec) detected while the BATSE onboard trigger was set for 5.5 overbackground in at least two detectors, in the energy range 50–300 keV. Among those we took the bursts for which $C_{max} = C_{min} = 1$ at the 1024 ms time scale, where C_{max} is the count rate in the second brightest illuminated detector and C_{min} is the minimum detectable rate. These constitute a group of 595 bursts. In our previous paper (Guetta et al. 2005) we have shown that the distribution of minimum rates is very narrow and we can take an average rate that corresponds to a threshold $P_{lim;BATSE}^{(50-300)keV} = 0.25 \text{ ph cm}^{-2} \text{ s}^{-1}$.

For Swift we consider all the long bursts detected until September 2006 (~130) bursts in the energy range 15–150 keV. Swift's complicated triggering algorithm is not based just on the concept of a minimal flux above the background. Still we can have an estimate of the effective Swift threshold by plotting in Fig. 1 the peak flux distribution. This figure compares the peak-flux cumulative distributions of the Swift GRBs with that of BATSE. The comparison is done in the energy band 50–300 keV, which is the band where BATSE detects GRBs. Note that for this comparison we have converted the BAT 15–150 keV peak fluxes to fluxes in the 50–300 keV band using the BAT peak fluxes and spectral parameters¹. We find an effective threshold of $P_{lim;Swift}^{(50-300)keV} = 0.18 \text{ ph cm}^{-2} \text{ s}^{-1}$ in agreement with what found by Górsak et al. (2004). Note that within the Swift band this threshold corresponds to $P_{lim;Swift}^{(15-150)keV} = 0.4 \text{ ph cm}^{-2} \text{ s}^{-1}$. The sensitivity of BeppoSax, HETE2 and Swift has been studied in detail by Band (2003, 2006). Band (2006) also studied the sensitivity of BAT instrument as a function of the combined GRB temporal and spectral properties. We refer to these papers for more details on these topics. The values of sensitivities used in this paper are in agreement with Band's results.

The method used to derive the luminosity function is essentially the one used by Schmidt (1999) and by Guetta et al. (2005). We consider a broken power law with lower and upper limits which are factors of $\lambda_1 = 1$ and λ_2 respectively times the break

¹ These parameters were taken from the Swift information page http://swift.gsfc.nasa.gov/docs/swift/archive/grb_table.html

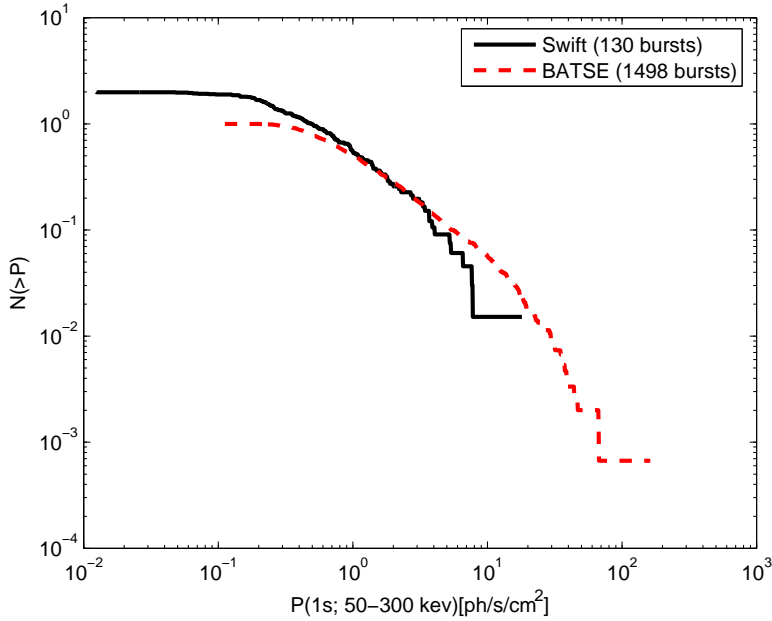


Fig.1. The observed BATSE and Swift peak flux cumulative distributions in the 50-300 keV energy range

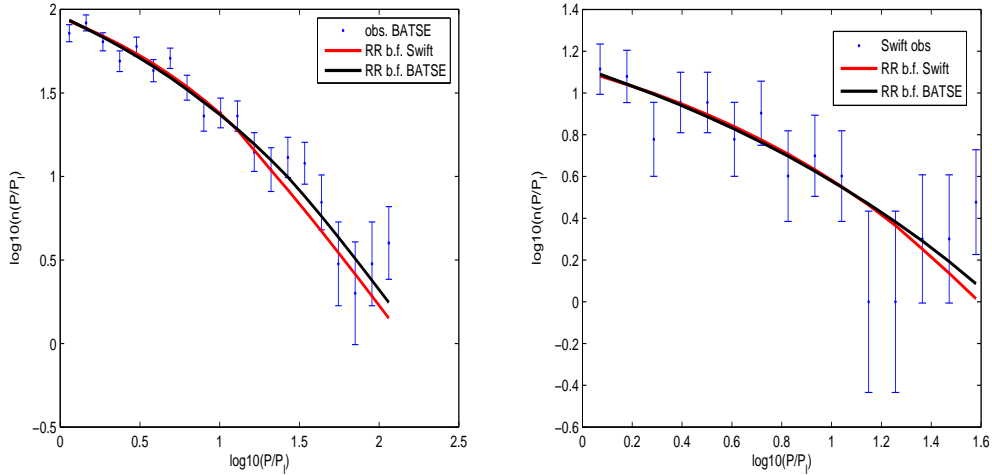


Fig.2. a) left panel: The predicted differential distribution $n(P/P_{\text{lim}})$ with the luminosity function parameters that best fit the BATSE sample (black curve) and the Swift sample (red curve) with a RR-SFR vs. the observed $n(C_{\text{max}}/C_{\text{min}})$ taken from the BATSE catalog. b) right panel: The predicted differential distribution $n(P/P_{\text{lim}})$ with the luminosity function parameters that best fit the BATSE sample (black curve) and the Swift sample (red curve) with a RR-SFR vs. the observed Swift $n(P/P_{\text{lim}})$ taken from the Swift catalog

luminosity L . The luminosity function (of the peak luminosity L) in the interval $\log L$ to $\log L + d\log L$ is:

$$f_L(L) = \begin{cases} \frac{8}{C_0} \frac{1}{L^2} & (L=L_1) \quad L_1 < L < L_2 \\ 0 & (L=L_2) \quad L_2 < L < 2L \end{cases}; \quad (1)$$

where c_0 is a normalization constant so that the integral over the luminosity function equals unity. We stress that the luminosity considered here is the "isotropic" equivalent luminosity, which is the one relevant for detection. It does not include a correction factor due to beaming.

Assuming that long GRBs follow the star formation rate we employ four parameterization of the star formation rate:

(i) Model SF2 of Porciani & Madau (2001):

$$R_{\text{GRB}}(z) = R_{\text{SF2}}(z) = \frac{23 \exp(3.4z)}{\exp(3.4z) + 22} \quad (2)$$

where $_{0}$ is the GRB rate at $z = 0$.

(ii) The Rowan-Robinson SFR (Rowan-Robinson 1999: RR-SFR) that can be fitted with the expression:

$$R_{\text{GRB}}(z) = \begin{cases} 0 & z < 1 \\ \frac{8}{10^{0.75z}} & z < 1 \\ 10^{0.75z_{\text{peak}}} & z > 1 \end{cases} \quad (3)$$

(iii) Model SF3 of Porciani & Madau (2001) with more star formation at early epochs:

$$R_{\text{GRB}}(z) = R_{\text{SF3}}(z) = \frac{16 \exp(3.4z - 0.4)}{\exp(-0.4)(\exp(2.93z) + 15)} \quad (4)$$

(iv) : The Star formation history parameter fit to the form of Cole et al. (2001) taken from Hopkins and Beacom (2006). This rate strongly declines with z at high redshift ($z > 4$)

(v) We consider a toy model where the rate is enhanced at high redshift and the transition is sharp. As mentioned earlier this model might be related to the lower metallicity at higher redshift. As a toy model we used a SFR as described in model (ii) but at $z > 2.5$ is enhanced by a factor of 2:

$$R_{\text{GRB}}(z) = \begin{cases} R_{\text{RR}}(z) & z < 2.5 \\ 3R_{\text{RR}}(z) & z > 2.5 \end{cases} \quad (5)$$

Note that this model resembles but is not the same as the one used by Natrajan et al. (2006) where there is just a jump in the rate and no association with the SFR at all (as not enough details about the model were given in that paper we could not reproduce it here).

(vi) For completeness we consider also a GRB rate that is in between of model (ii) and

(v)

$$R_{\text{GRB}}(z) = \begin{cases} R_{\text{RR}}(z) & z < 2.5 \\ 2R_{\text{SF2}}(z) & z > 2.5 \end{cases} \quad (6)$$

We use the standard cosmological parameters $H_0 = 65 \text{ km s}^{-1} \text{ Mpc}^{-1}$, $\Omega_m = 0.3$, and $\Omega_\Lambda = 0.7$. The different rates are shown in Fig 3.

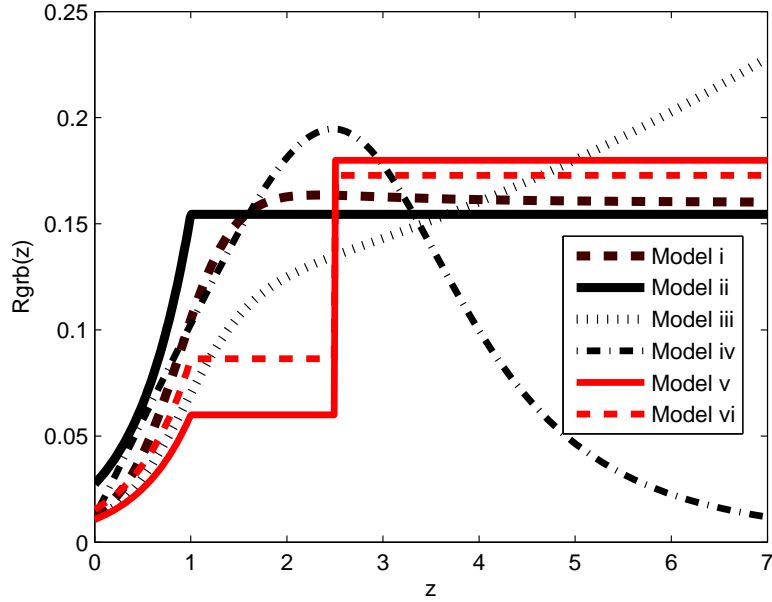


Fig. 3. The star formation histories considered in the paper

An important factor in the modelling is the cosmologicalk correction. We approximate the typical effective spectral index in the observed range of 50 keV to 300 keV as $(N(E)/E)^{1/6}$. This value that was calculated by Schmidt (2001) for BATSE bursts is also adequate for Swift bursts whose average spectral index is 1.5. The use of this average correction is justified when we compare estimates of the luminosity based on this average value and on the real spectrum (see Fig. 4 below.)

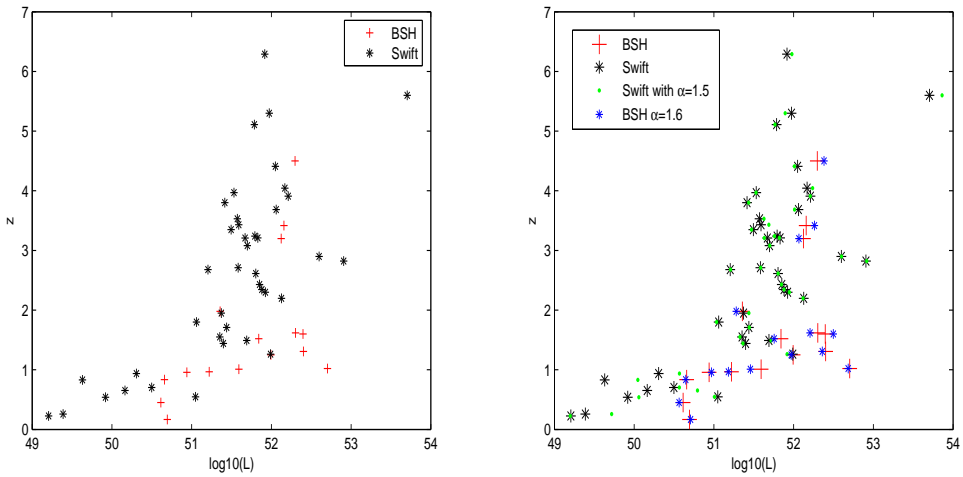


Fig. 4. a), left panel: the luminosities and redshifts of the BeppoSAX / HETE 2 (BSH in the legend) sample compared with the Swift sample. b), right panel: the same as left panel, also marked are the values of L extrapolated using the average photon index for each sample.

The number of bursts with a peak $ux > P$ is given by:

$$N > P = \int_0^{\infty} \phi(L) d\log L \int_0^{z_{\max}(L, P)} \frac{R_{\text{GRB}}(z)}{1+z} \frac{dV(z)}{dz} dz$$

where the factor $(1+z)^{-1}$ accounts for the cosmological time dilation and $dV(z)=dz$ is the comoving volume element.

In principle one should perform a maximum likelihood analysis to obtain the best values of the luminosity parameters to fit both the BATSE and the Swift samples. However, a simpler approach is sufficient as it gives a consistent fit. We vary the luminosity function parameters α , β , and L_0 keeping $\alpha_1 = 100$ and $\alpha_2 = 100$ and inspect the quality of the fit to the observed BATSE peak ux distribution. Once we obtain the best fit parameters for the BATSE sample we test the quality of the fit with both the observed BATSE and the Swift peak ux distributions. We then repeat the same procedure and look for the luminosity function parameters that best fit the Swift sample. Then we check the quality of the fit with these parameters with the observed BATSE and the Swift peak ux distributions. In Figure 2a (2b) we show a comparison of the observed differential distributions $n(P) = dN/dP$ of BATSE (Swift) with the predicted distribution obtained with the RR-SFR model (ii) for the parameters that best fit the BATSE (Swift) data. On the same figure also depicted is the curve obtained using the parameters that best fit the Swift (BATSE) data. Similar curves are obtained for the other models. The χ^2 -square values reported in Table I show the consistency between the Swift and BATSE peak ux samples. The consistency is reassuring. However the fact that we obtain good fits for the data with very different models for the GRB rates reflects the insensitivity, noticed already by Cohen and Piran (1995), of the peak ux distribution to the details of the GRB rate. The peak ux distribution is a convolution of the luminosity function and the GRB rate and different assumptions on the rate simply result in different luminosity function.

The results of the fit are reported in Table 1. These show that the best fit parameters and α are rather robust and they do not depend on the exact shape of the GRB rate chosen and the values of α and β found for these rather different models are all within the errorbars of each other. To obtain the local rate of GRBs per unit volume, ϕ , we need to estimate the effective full-sky coverage of the GRB samples. For BATSE we use 595 (47% of the long GRBs) events detected over 1386 days in the 50–300 keV channel with a sky exposure of 48%. For Swift we consider 130 bursts detected in 1.5 yr and a sky coverage is 1/6. The value of L_0 is around 2.5×10^{51} erg/sec. It is somewhat higher for models (v) and (vi), as expected because in these cases the intrinsic distribution is farther, and hence stronger pulses are needed. The local rate varies, however by a factor of 5 from the "farthest" models (v) and (vi) to the nearest one (ii). Similarly the fraction of expected high redshift ($z > 6$) Swift bursts vary strongly among the different models: (i) 1.3%, (ii)

0.67% (iii) 3.5% , (iv) 0.07% , (v) 6.2% and (vi) 6.0%. These numbers are somewhat lower than what was previously expected (Volker & Loeb 2006).

The somewhat arbitrary values of $L_{1,2} = (100, 100)$ are chosen in such a way that even if there are bursts less luminous than $L = L_1$ or more luminous than L_2 they will constitute only a very small fraction (less than 1%) of the observed bursts. Bursts above $L = L_2$ are very bright and are detected to very large distances. However, such strong bursts are very rare. Increasing L_2 does not add a significant number of bursts (observed or not) and this does not change the results. In particular it does not change the overall rate. L_1 is more subtle. The luminosity function increases rapidly with decreasing luminosity. Thus, a decrease in L_1 has a strong effect on the overall rate of GRBs. However, most of the bursts below $L = L_1$ are undetectable by current detectors, unless they are extremely nearby. Even if the luminosity function continues all the way to zero, this will increase enormously the overall rate of the bursts (Guetta & Piran 2006; Guetta & Della Valle 2006) (which will in fact diverge in this extreme example) however most of these additional weak bursts will be undetected and the total number of detected bursts won't increase.

model-sample	Rate (z=0) G pc ⁻³ yr ⁻¹	L 10 ⁵¹ erg/sec			$\chi^2_{\text{b:f}}$	χ^2_{other}
(i)-BAT SE	$0.07^{+0.1}_{-0.05}$	$5.5^{+2.1}_{-3.1}$	$0.3^{+0.3}_{-0.2}$	$2^{+1}_{-0.5}$	0.82	1.2
(i)-Swift	$0.10^{+0.08}_{-0.06}$	$3.3^{+3.1}_{-1.0}$	$0.1^{+0.5}_{-0.05}$	$2^{+0.8}_{-0.4}$	0.85	1.0
(ii)-BAT SE	$0.18^{+0.21}_{-0.1}$	$5.5^{+2.1}_{-3.7}$	$0.4^{+0.2}_{-0.3}$	$2.5^{+0.5}_{-1}$	0.86	1.1
(ii)-Swift	$0.27^{+0.15}_{-0.22}$	$2.3^{+5.1}_{-0.3}$	$0.1^{+0.5}_{-0.05}$	$2^{+0.4}_{-0.5}$	0.81	0.97
(iii)-Swift	$0.1^{+0.05}_{-0.03}$	4^{+2}_{-1}	$0.1^{+0.3}_{-0.03}$	$2^{+1}_{-0.2}$	0.82	1.1
(iv)-Swift	$0.11^{+0.08}_{-0.04}$	$3.0^{+1.9}_{-2.8}$	$0.2^{+0.3}_{-0.1}$	$2^{+0.7}_{-0.5}$	0.83	1.2
(v)-Swift	$0.05^{+0.03}_{-0.03}$	$6.5^{+0.8}_{-2}$	$0.2^{+0.3}_{-0.1}$	$1.7^{+0.5}_{-0.3}$	0.85	1.2
(vi)-Swift	$0.07^{+0.03}_{-0.04}$	$6.5^{+0.8}_{-2}$	$0.2^{+0.3}_{-0.1}$	$2^{+0.2}_{-0.3}$	0.9	1.2

Table 1. Best parameters Rate (z = 0), L, and and their 1- confidence levels.

For each we report the χ^2 values corresponding to the best t ($\chi^2_{\text{b:f}}$). Also shown are the χ^2 values for the t to the BAT SE (Swift) data obtained using the parameters that best fit the Swift(BAT SE) sample (χ^2_{other}).

3. The redshift distributions

We turn now to the observed redshift distributions of BeppoSAX/HETE 2 and Swift. For BeppoSax/HETE 2 we consider the observed distribution of all the bursts with an available redshift: 32 bursts from <http://www.mpe.mpg.de/~jcg/grbgen.html> (excluding GRB 980425 with $z = 0.0085$). For Swift we consider all the bursts with an available redshift: 39 bursts from the Swift home page. It is hard to quantify the selection effects

that arise in the determination of the redshift. The problem is most severe if the redshift determination depends on the identification of emission lines in the spectrum of the host galaxy. Since there are very few emission lines in the range $1.3 < z < 2.5$ (Hogg & Fruchter, 1999) such redshifts may be missed. For BeppoSAX/HETE2 this is the main mode of redshift identification. We follow Hogg & Fruchter (1999) and consider a modelled distribution in which all the GRB with optical afterglow but without measured redshift are assigned to be in this redshift range $1.3 < z < 2.5$. Using the data in <http://www.mpe.mpg.de/~jbg/grbgen.htm> we have a sample of 46 BeppoSAX/HETE2 GRBs with no measured redshifts which we assign to this range. The situation concerning *Swift*'s bursts is more complicated as most *Swift* redshifts are obtained using absorption lines, for which the main selection effect is the weakness of the afterglow signal or the optical depth within the host (Fiore et al. 2006). Both selection effects work against high redshift bursts. Lacking any reasonable model we consider for *Swift* just the observed data set.

Figure 4 depicts the isotropic peak luminosities and redshifts of the BeppoSAX/HETE2 and *Swift* samples. This figure shows clearly the differences in thresholds. In the second figure we also plot the values of L for the average photon index assumed in the calculations. As we can see from this figure the values of the peak luminosities obtained using the average spectrum are rather similar to the ones obtained using the real spectrum. Therefore, it is reasonable to use the average spectrum for the k -correction as we have done in this analysis. Another feature seen in this figure is that the *Swift* redshift distribution shows (seen even more clearly in Fig. 5) a paucity of bursts in the range $1 < z < 2$. It is not clear if this is statistically significant, but it is very apparent in the data. There is no clear selection effect that could give rise to this feature.

Using the different models for the GRB rate and the luminosity function we derive now the expected distribution of the observed bursts' population:

$$n(z; L) dz d\log(L) = \frac{R_{GRB}(z) dV(z)}{1+z} \circ(L) d\log L : \quad (7)$$

The expected redshift distribution is:

$$N(z) = \frac{R_{GRB}(z) dV(z)}{1+z} \int_{L_{min}(P_{lim}; z)}^{L_{max}} \circ(L) d\log L ; \quad (8)$$

where $L_{min}(P_{lim})$ is the luminosity corresponding to minimum peak flux P_{lim} for a burst at redshift z and $L_{max} = L_{z=2} = 10L$. This minimum peak flux corresponds to the detector's threshold. For BeppoSax/HETE2 we use, $P_{lim}^{(50-300)keV} = 0.5 \text{ ph cm}^{-2} \text{s}^{-1}$, which is roughly the limiting flux for the GRBM on BeppoSAX (Guidorzi Ph.D thesis). The triggering algorithm for *Swift* is rather complicated but as shown in Fig. 1 it can be approximated by a minimum rate: $P_{lim \text{ Swift}}^{(50-300)keV} = 0.18 \text{ ph/cm}^2/\text{sec}$.

Our results are summarized in Table 2 and in Figs. 5 and 6 in which we present a comparison of the observed (corrected and uncorrected) BeppoSAX/Hete2 and *Swift*

redshift distributions with theoretical models that were obtained from best fits of the model's parameters to the Swift peak flux distribution. Qualitatively similar results are obtained from best fits to the BATSE peak flux distribution. Fig. 5 depicts the differential distribution of the observed redshifts while Fig. 6 depicts the integrated distribution. The values of the KS test for the different models are shown in Table 2. The most remarkable feature is that none of the pure SFR models (i-iv) is consistent with the Swift data. This result is consistent with what found in Daigne et al. 2006. Additionally, it was very difficult to find models that fit both the Swift and the BeppoSAX/HETE2 data. Models (i), (iii) and (iv) that favor a nearer GRB distribution, are consistent with the BeppoSAX/HETE2 distribution while model (v) that favors a more distant distribution is consistent with the observed Swift redshift distribution. The only combined fit to both data sets is obtained for Model (vi) which is consistent with the Swift distribution (KS values = 0.19) and with the corrected the BeppoSAX/HETE2 data (KS values = 0.17). Model (vi) represents a variation of the rather arbitrary parameters of model (v). Clearly, we can consider a series of models based on RR SFR ranging from no enhancement at high z (model ii) which fits the uncorrected BeppoSAX/HETE2 sample to a very strong enhancement at high z (model v) that fits just the Swift data. In model (vi) we consider an intermediate enhancement which is formally consistent with both the Swift and the modelled BeppoSAX/HETE2 data. However, as we discuss later, even in these models and even in the models like, (i), (ii), (iv) that are compatible with BeppoSAX/HETE2 redshift distribution, the two dimensional redshift luminosity distribution shows too many high luminosity bursts. Note that similar results were obtained when we modelled SF2 by adding an ad hoc enhancement at large redshift.

model	KS test		KS test with Swift z
	with BeppoSAX/HETE2 z	with BeppoSAX/HETE2 z corr	
(i)	0.04	0.69	< 0.01
(ii)	0.63	0.03	< 0.01
(iii)	0.01	0.27	0.03
(iv)	0.25	0.41	< 0.01
(v)	< 0.01	0.05	0.85
(vi)	0.03	0.17	0.19

Table 2. KS probability values for the BeppoSax/HETE II (BeppoSAX/HETE2) and the Swift sample for the luminosity function parameters that best fit the Swift peak flux distribution

Fig. 7 depicts a comparison of the two dimensional redshift and luminosity distributions between the BeppoSAX/HETE2 data and model (ii). Naturally, we include here only bursts with known redshifts. Several features are apparent. First, the estimate of

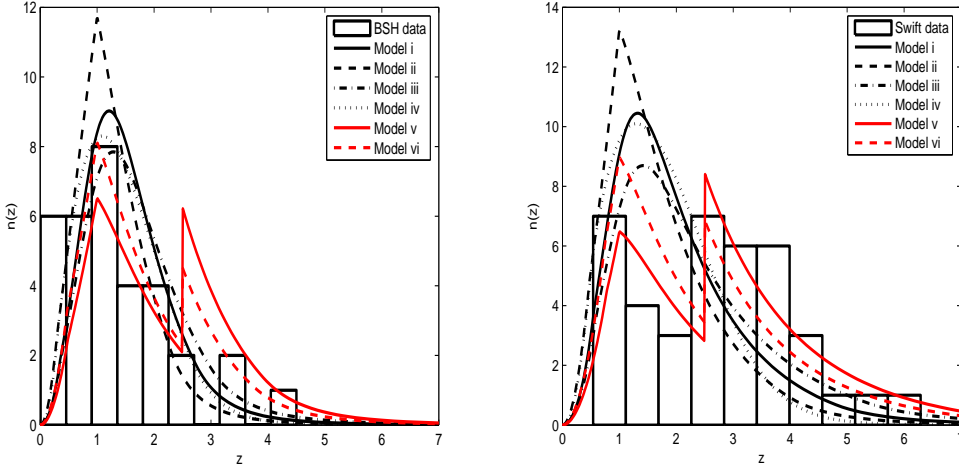


Fig. 5. The predicted and the observed differential distributions of the GRBs redshift for the different models (a) left panel – Swift data with theoretical models with $P_{\text{lim}} = 0.18$ (b) right panel BepoSax/HETE 2 (BSH in the legend) and the models with $P_{\text{lim}} = 0.5$.

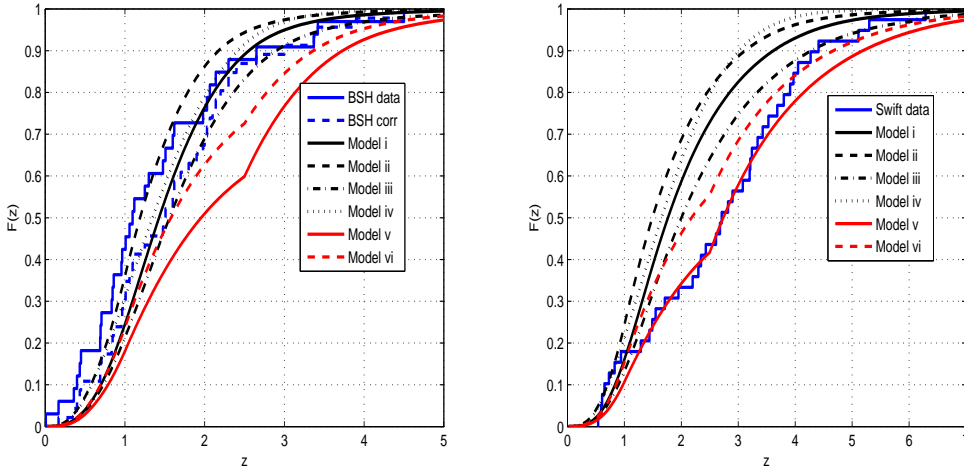


Fig. 6. The predicted and the observed cumulative distributions of the GRBs redshift for the different models (a) left panel – Swift data with theoretical models with $P_{\text{lim}} = 0.18$ (b) right panel BepoSAX / HETE 2 and the models with $P_{\text{lim}} = 0.5$. For BepoSAX / HETE 2 we also show the distribution where selection effects are taken into account assuming that all the GRB with no redshift but with optical afterglow lie in the range $1.3 < z < 2.5$.

$P_{\text{lim}} = 0.5$ for BepoSAX / HETE 2 is reasonable. Only one burst is detected in the "forbidden" region with a lower peak flux. However, it is clear that there is no good fit between the model and the observed distribution. The lack of bursts in the range $1.5 < z < 3$ may be explained by selection effects. However, in addition, there are significantly more high luminosity bursts than predicted by the model. It is clear that even though the KS test of the integrated redshift distribution for this model suggests that the model is

consistent with the observed distribution the two dimensional distribution of luminosities and redshifts is inconsistent. Similar, or worse results are obtained for this data with all other models that we have considered including, in particular, model (vi).

A similar comparison between model (v) and the Swift data is shown in Fig 8. Here there are several bursts in the forbidden region in the upper left part of the plot where the peak flux is below $0.18 \text{ ph/cm}^2/\text{s}$. These bursts reflect the fact that Swift's trigger is not based just on peak flux counts. However as these bursts cluster very close to the line $P_{\text{lim}} = 0.18 \text{ ph/cm}^2/\text{s}$ we find that the complicated triggering algorithm of Swift is not an issue. The fit of the observed data to the model is clearly better than the one seen in Fig. 7. Still it is not compelling. Here the basic problem can be seen also in Fig. 5 that depicts the observed differential redshift distribution of Swift bursts. The paucity of bursts in the range $1 < z < 2$ hints towards a two population model – or towards a high redshift enhancement of the sort that we have crudely modeled in (v). Unlike the BeppoSAX/HETE2 sample we don't see here a significant fraction of high luminosity bursts (as compared with the model) but again there are hints towards a broader luminosity function than the one we use.

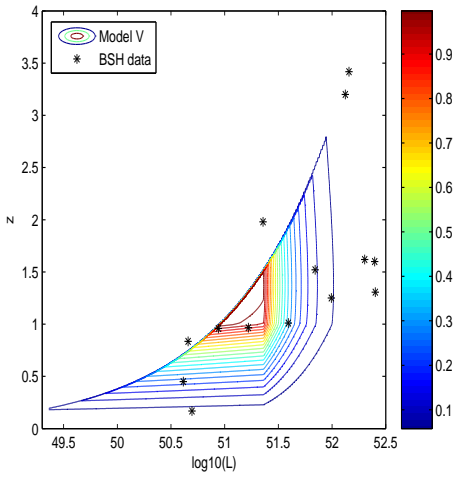


Fig. 7. The two dimensional probability distribution of expected redshift and luminosity for the luminosity function parameters that best fit the Swift peak flux distribution considering a RR-sfr and $P_{\text{lim}} = 0.5 \text{ ph/cm}^2/\text{s}$. Contour lines are 0.9, 0.8... 0.01 of the maximum. Also marked are the BeppoSax/HETE2 (BSH in the legend) GRBs with a known redshift and spectral index. Note that there is only one burst in the "forbidden" region in the upper left part of the plot where the peak flux is below $0.5 \text{ ph/cm}^2/\text{s}$.

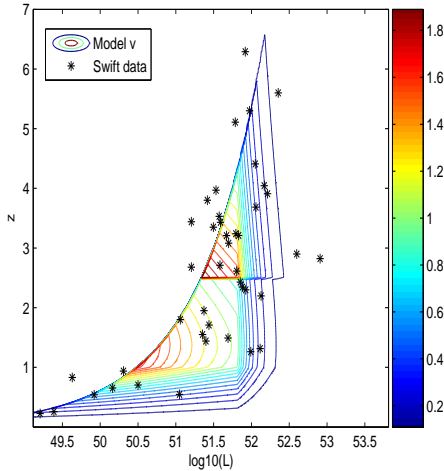


Fig. 8. The two dimensional probability distribution of expected redshift and luminosity for the luminosity function parameters that best fit the Swift peak flux distribution considering model (v) and $P_{\text{lim}} = 0.18 \text{ ph/cm}^2/\text{s}$. Contour lines are 0.9, 0.8... 0.01 of the maximum. Also marked are the Swift GRBs with a known redshift. Note that there are several bursts in the "forbidden" region in the upper left part of the plot where the peak flux is below $0.18 \text{ ph/cm}^2/\text{s}$. These bursts reflect the fact that Swift's trigger is not based just on peak flux counts. However as these bursts cluster very close to the line $P_{\text{lim}} = 0.18 \text{ ph/cm}^2/\text{s}$ we find that the complicated triggering algorithm of Swift is not an issue here.

4. Conclusions and Implications

We find that Swift GRBs do not follow the SFR as described by several different models (i-iv). Given these SFRs there is no luminosity function that can fit both the Swift observed peak flux and the z -distributions. We were able to obtain a reasonable fit when we considered a GRB rate function that included a high redshift enhancement. This might be related to suggestions that long GRBs arise preferably in low metallicity regions (Fynbo et al 2003; Vreeswijk et al, 2004). But it could arise from other reasons. We used a simple toy scheme to model this enhancement. Because of the very crude nature of the model and the limited scope of the available data we did not try to optimize extensively the parameters of this model. It was reassuring that we obtained a reasonable fit with such a simple model and without an extensive search for the parameters. It is remarkable that the enhancement arises in the high redshift range, where the bursts and their afterglow are weaker and hence selection effects are expected to reduce rather than increase the number of bursts with detected redshifts.

We mention now the strange paucity of Swift bursts with $1 < z < 2$. If real and not just a statistical fluctuation or a result of some unknown selection effect this paucity may indicate: (a) A jump in long GRB rate or another factor at higher redshifts; (b)

A dependence of the luminosity function on the rate or even the existence; (c) The appearance of two populations one at lower redshift and another one at higher redshifts (which can be viewed as a special case of a z dependence of the luminosity function). While these speculations are intriguing it is clear that it is essential to determine the selection effects that control the samples of GRBs with determined redshifts before far reaching conclusions are made.

The only GRB rate and luminosity functions that are consistent with these distributions and with both observed redshift distributions (of BeppoSAX/HETE2 and of Swift) is a one with an enhanced GRB rate at large redshift. This consistency is achieved only after we modified the BeppoSAX/HETE2 sample by adding all bursts with no redshift in the range $1.5 < z < 2.5$ in which there are no strong emission lines and redshift identification is difficult (Hogg & Fruchter, 1999). However, as the two dimensional distribution of redshifts and luminosities of the BeppoSAX/HETE2 does not seem to fit the model we do not assign a great significance to this fact.

Another important result is that the BATSE and Swift peak flux distributions are consistent with each other and with the estimated limiting fluxes for detection for the two detectors. The combined analysis suggests that the local rate of GRBs (without a beaming correction) can be determined up to a factor of approximately five and it ranges between $0.05 \text{ Gpc}^3 \text{ yr}^{-1}$ for a rate function that has a large fraction of high redshift bursts to $0.27 \text{ Gpc}^3 \text{ yr}^{-1}$. Note that the inferred low local rates, $0.05 \text{ Gpc}^3 \text{ yr}^{-1}$, which are about an order of magnitude lower than previous estimates (Guetta, Piran & Waxman, 2005), arise from the models that involve metallicity enhancement at large redshifts. These rates do not include the beaming correction which is of order 100. Even with this correction these rates correspond to a local rate of a burst per 2×10^6 years per galaxy, indicating that strong GRBs are a very rare phenomenon. However, the actual rate of weak bursts could be much higher if indeed there is a large population of very low luminosity bursts, as inferred from the detection of GRB 060218 (Soderberg et al., 2006). These models predict, on the other hand, a relatively large fraction of about 6% of high redshift ($z > 6$) Swift bursts.

When considering the BeppoSAX/HETE2 redshift distribution on its own it seemed that even luminosity functions and rates that fit the peak flux distribution and the observed redshift distributions do not fit the two dimensional luminosity and redshift distribution. The paucity of bursts with redshifts between $1.5 < z < 2.5$ can be explained by the selection effect mentioned earlier. However, the excess of very luminous low redshift bursts is unexpected and indicates that other selection effects that favor identification redshift determination of such bursts take place and possibly dominate the BeppoSAX/HETE2 sample. If correct this has potential implications to other statistical information that has been determined from this data sample.

References

Band, D., 2003, *ApJ* 588, 945.

Band, D., 2006, *ApJ* 644, 378.

Cohen E., Piran T., 1995, *ApJ*, 444, L25

Cole, S. et al., 2001, *MNRAS* 326, 255.

Daigne, F., Rossi, E. M. & Mochovitch, R., 2006, *MNRAS* 373, 1034.

Fenimore, E. & Bloom, J., 1995, *ApJ* 453, 25

Fiori, F., Guetta, D., Piranomonte, S., D'Elia, V. & Antonelli, A. [astro-ph/0610740](#) Nuovo Cimento in press.

Fynbo, J. et al., 2006, *A&A* 451, L47.

Fynbo, J. et al., 2003, *A&A* 406, L63.

Guetta, D., Piran, T. & Waxman E., 2005, *ApJ*, 619, 412. (GPW).

Guetta, D. & Piran, T., 2005, *A&A*, 435, 421.

Guetta, D. & Piran, T., 2006, *A&A*, 453, 823.

Guetta, D. & Della Valle, M., 2006, *ApJ* in press.

Hogg, D. & Fruchter, A., 1999, *ApJ* 520, 54.

Hopkins, A. M. & Beacom, J. F., 2006, *ApJ* 651, 142.

Horack, J. M. & Hakkila, J., 1997, *ApJ* 479, 371.

Loredo, T. & Wasserman, Ira M., 1998, *ApJ* 502, 75L

Natarajan, P. et al., 2005, *MNRAS* 364, L8.

Pettini, M. et al., 2003, *ApJ* 594, 695.

Piran, T., 1992, *ApJ* 389, L45.

Porciani, C., and Madau, P., 2001, *ApJ* 548, 522.

Rice, P. A. et al. 2005, *GRB Circular Network*, 3612, 1.

Rowan-Robinson, M., 1999, *Ap&SS* 266, 291R.

Schmidt, M., 1999, *ApJ* 523, L117.

Schmidt, M., 2001, *ApJ* 559, L79.

Sethi, S. & Bhargavi, S. G., 2001, *A&A* 376, 10S.

Soderberg, A., et al., 2006, *Nature*, 442, 1014.

Volker, B. & Loeb, A., 2006, *ApJ* 642, 382.

Vreeswijk, P. M., Moller, P. & Fynbo, J. P. J., 2003, *A&A* 409, L5.